



**HAL**  
open science

# Instabilités oscillatoires d'un cylindre libre confiné entre deux plaques sous le seuil d'émission de tourbillons de Von Karman

Harold Auradou, Jean-Pierre Hulin, Veronica d'Angelo, Luciano Gianorio, Benoit Semin, Mario Cachile

## ► To cite this version:

Harold Auradou, Jean-Pierre Hulin, Veronica d'Angelo, Luciano Gianorio, Benoit Semin, et al.. Instabilités oscillatoires d'un cylindre libre confiné entre deux plaques sous le seuil d'émission de tourbillons de Von Karman. CFM 2013 - 21ème Congrès Français de Mécanique, Aug 2013, Bordeaux, France. hal-03439805

**HAL Id: hal-03439805**

**<https://hal.science/hal-03439805>**

Submitted on 22 Nov 2021

**HAL** is a multi-disciplinary open access archive for the deposit and dissemination of scientific research documents, whether they are published or not. The documents may come from teaching and research institutions in France or abroad, or from public or private research centers.

L'archive ouverte pluridisciplinaire **HAL**, est destinée au dépôt et à la diffusion de documents scientifiques de niveau recherche, publiés ou non, émanant des établissements d'enseignement et de recherche français ou étrangers, des laboratoires publics ou privés.

# Oscillating instability of free and tethered confined cylinders at low Reynolds numbers

V. D'ANGELO<sup>a</sup>, L. GIANORIO<sup>a</sup>, M. CACHILE<sup>a</sup>, H. AURADOU<sup>b</sup>, J.P. HULIN<sup>b</sup>, B. SEMIN<sup>c</sup>

a. Grupo de Medios Porosos, Facultad de Ingeniería, Paseo Colon 850, 1063, Buenos Aires (Argentina), CONICET (Argentina).

b. Univ Pierre et Marie Curie-Paris 6, Univ Paris-Sud, CNRS, F-91405. Lab FAST, Bât 502, Campus Univ, Orsay, F-91405 (France).

c. Lab. LPS, Département de Physique de l'ENS, 24 rue Lhomond, 75231 Paris Cedex 05.

## Résumé :

*On observe l'instabilité oscillatoire d'un cylindre horizontal (diamètre  $D$ ) dans un écoulement vertical de vitesse  $U$  entre deux plaques parallèles (distance  $H$ ) pour des rapports  $D/H \gtrsim 0.45$ . Des oscillations transverses aux plaques se produisent à partir de nombre de Reynolds  $Re \simeq 20$  nettement plus faibles que pour l'émission de tourbillons derrière des cylindres fixes dans la même géométrie. Pour des cylindres libres, la fréquence  $f$  des oscillations est presque indépendante de  $D/H$  et de la longueur  $L_c$  du cylindre et est déterminée par une vitesse relative  $V_r$  du cylindre et du fluide. Pour un cylindre libre, comme pour un cylindre tenu par des fils de suspension, le nombre de Strouhal  $fH/V_r$  décroît lentement avec le nombre de Reynolds  $V_r H/\nu$  de manière indépendante de la densité et de la viscosité du fluide.*

## Abstract :

*An oscillatory instability is observed for an horizontal cylinder (diameter  $D$ ) in a vertical flow of velocity  $U$  between parallel plates (distance  $H$ ) for ratios  $D/H \gtrsim 0.45$ . Oscillations transverse to the plates occur down to Reynolds numbers  $Re \simeq 20$ , i.e. significantly below those for vortex shedding behind fixed cylinders in such geometries. For free cylinders, the frequency  $f$  of the oscillations is nearly independent of  $D/H$ , of the length  $L_c$  of the cylinder and is determined by a relative velocity  $V_r$  of the cylinder and the fluid. For both a free and a tethered cylinder, the Strouhal number  $fH/V_r$  decreases slowly with the Reynolds number  $V_r H/\nu$  following a law independent of the fluid density and viscosity.*

**Mots clefs :** oscillation, cylinder, confined

## 1 Introduction

The motion of elongated particles and fibers in a fluid flowing in a confined geometry (ducts, pores, microchannels) is of interest in many industrial and natural flows. We study here a horizontal rigid cylinder placed between two parallel planes inside which a vertical flow is established. Up to recently, research in this configuration dealt mainly with the determination of the force on a cylinder extending across the channel [2] or a part of it [4] and on vortex shedding behind it [3].

The present paper deals specifically with the occurrence of instabilities for cylinders shorter than the width of the cell. One uses both tethered cylinders moving only in the direction transverse to the cell walls and free cylinders which can translate in all three directions of space, rotate about their axis and have a varying angle  $\theta$  with respect to the horizontal. Of special interest are the dependence of the instabilities on the geometry of the cylinder (length, diameter), on the comparison between free or tethered cylinders and on the velocity and viscosity of the flowing fluid.

## 2 Experimental setup and procedure

The experimental setup consists of plexiglas Hele Shaw cells placed vertically (Fig. 1). Two different cells have been used : their height, width and aperture are respectively  $L = 350$ ,  $W = 100$  and  $H = 3$  mm (cell #1) and  $L = 290$ ,  $W = 90$  and  $H = 2.85$  mm (cell #2). The vertical sections of the cell have a Y-shape in their upper part ; the upper end of the cell is at the bottom of a rectangular bath with a slit allowing for the flow of the fluid and the insertion of the cylinders.

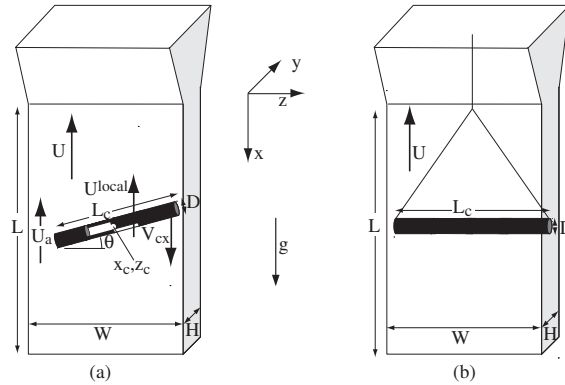


FIGURE 1 – Experimental setup. a) Free cylinder :  $U$  : mean flow velocity,  $V_{cx}$  : vertical component of the cylinder velocity. b) Tethered cylinder.

An upward flow may be imposed by a gear pump : the mean fluid velocity  $U$  is counted in this case as negative and varies between 0 and  $-25$  mm/s. The flowing fluid is either a water-glycerol solution of concentration in weight ranging between 0 and 20%, a water-salt-glycerol solution or a water-natrosol solution ; the concentration of the water-salt-glycerol solutions is adjusted so that  $\rho_f = 1.035$  g/cm<sup>3</sup> the viscosity and density of the solutions at the different concentrations are listed in Tab. 1.

TABLE 1 – Physical properties of the solutions used in the experiments at a temperature  $T = 25^\circ C$ . Concentration in weight of glycerol (or natrosol) :  $C$  ; density :  $\rho_f$  ; dynamical viscosity :  $\mu$ .

Name	$C$ (%)	$\rho_f$ (g/cm <sup>3</sup> )	$\mu$ (mPa.s)
Water-glycerol solutions			
W	0	0.997	0.893
WG5	5	1.008	1.010
WG10	10	1.02	1.153
WG15	15	1.032	1.331
WG20	20	1.044	1.542
Water-salt-glycerol solutions			
WS	0	1.035	0.95
WGS5	5	1.035	1.05
WGS10	10	1.035	1.17
WGS15	10	1.035	1.33
Water-natrosol solutions			
WN1	0.1	0.998	1.11
WN2	0.2	0.998	2.2

Most experiments use plexiglas cylinders with a density  $\rho_s = 1.2 \pm 0.05 \times 10^3$  kg/m<sup>3</sup>, a diameter to aperture ratio  $0.36 \leq D/H \leq 0.78$  and a length to cell width ratio  $0.11 \leq L_c/W \leq 0.95$ . A few experiments were performed using carbon cylinders of higher density  $\rho_s = 1.54 \pm 0.05 \times 10^3$  kg/m<sup>3</sup>. In the

“tethered” configuration, the two ends of the cylinders are attached by 0.1 mm nylon threads to a fixed suspension point located close to the inlet. In the “free” case, the cylinder is initially horizontal in the upper bath ( $\theta = 0$ ) and moves down into the constant aperture section : the location of the cylinder at the beginning of the measurement is adjusted by varying the flow rate [1].

The motion of free cylinders is monitored by a digital camera facing the plane  $(x, z)$  of the cell walls (the  $x$  axis is vertical and oriented downwards); for tethered cylinders, one observes instead the plane  $(x, y)$  of the aperture. The typical resolution of the images is 0.3 mm/pixel with  $1024 \times 768$  pixels and the frame rate is 30 *fps*. Processing digitally the images of the cylinder provides the coordinates  $(x_c, z_c)$  of its center of mass and its angle  $\theta$  with respect to the horizontal. Staggered stripes parallel to the length are painted on the center part of the cylinder in order to detect its rotation around the axis (angular oscillations synchronous with the transverse ones and allows one to detect them). The transverse displacement of the tethered cylinders is directly measured in the  $(y, z)$  plane.

### 3 Experimental results

#### 3.1 Flow regimes and mean motion of free cylinders

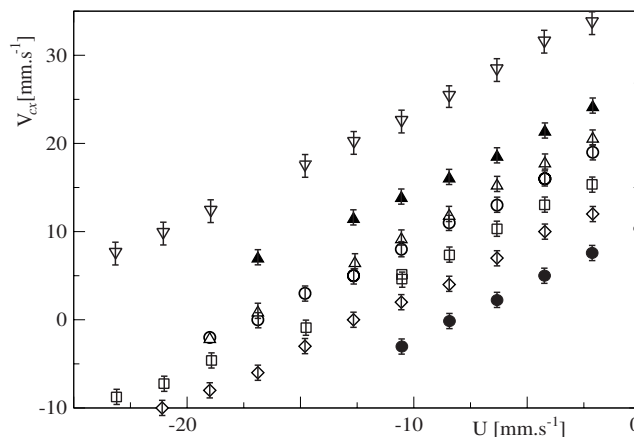


FIGURE 2 – Vertical velocity  $V_{cx}$  of free cylinders of diameter  $D$  in solutions *WN1* or *WN2* (see Tab. 1) as a function of the fluid velocity  $U$ . Open symbols : oscillating cylinders; solid symbols : no oscillations. plexiglas cylinders ( $\rho_s = 1.20 \text{ g.cm}^{-3}$ ) - ( $\Delta$ ), ( $\blacktriangle$ ) :  $D = 1.5 \text{ mm}$  ( $D/H = 0.53$ ), *WN1*; ( $\circ$ ), ( $\bullet$ ) :  $D = 1.6 \text{ mm}$  ( $D/H = 0.56$ ), *WN1* for ( $\circ$ ) and *WN2* for ( $\bullet$ ); ( $\square$ ) :  $D = 1.8 \text{ mm}$  ( $D/H = 0.63$ ), *WN1*; ( $\diamond$ ) :  $D = 2.1 \text{ mm}$  ( $D/H = 0.74$ ), *WN1*. Carbon cylinder ( $\rho_s = 1.54 \text{ g.cm}^{-3}$ ) - ( $\nabla$ ) :  $D = 1.5 \text{ mm}$  ( $D/H = 0.53$ ), *WN2*.

For free cylinders, the mean vertical velocity  $V_{cx}$  of the cylinders has been studied as a function of the velocity  $U$  for different cylinder diameters and lengths and different fluid viscosities (Fig. 2). On the one hand, the variation is always linear as long as  $U < 0$  and the slope  $\alpha$  of the variation remains equal to  $1.4 \pm 0.05$  for different values of  $D$ ,  $L_c$ ,  $\eta$  or  $\rho_s$ . The value  $\alpha \neq 1$  reflects likely the different velocity fields created when the cylinder moves or when one creates a Poiseuille flow by injecting a fluid. On the other hand, the different lines are shifted with respect to one another so that, in particular, the flow velocity  $U$  at which the cylinder remains at rest depends on the above parameters : the corresponding absolute value of  $U$ , referred to in the following as  $V_r$ , is determined from the linear fit with the data.

The flow regime observed depends largely on the ratio  $D/H$  : no oscillation takes place at low  $D/H$  values (typ.  $D/H \leq 0.4$ ) For  $0.46 \leq D/H \leq 0.56$ , pure transverse oscillations are observed with the cylinder remaining generally horizontal. For  $D/H \gtrsim 0.6$ , a lower frequency flutter in the  $(x, z)$  plane appears, producing oscillations of the angle  $\theta$  with respect to the horizontal and of the lateral coordinate  $z_c$  of the center of mass. These oscillations are still observed at larger  $D/H$  ratios ( $D/H \simeq 0.8$ ) while the transverse ones disappear.

### 3.2 Transverse oscillations for tethered and free cylinders

The variation of the frequency of the oscillations as a function of the flow velocity  $U$  for a free cylinder is displayed in Fig. 3 for cylinders of same length  $L_c = 55$  mm and of different diameters  $1.3 \leq D \leq 1.6$  mm ( $0.46 \leq D/H \leq 0.56$ ). The frequency is remarkably independent of  $D/H$  and varies only weakly with  $U$ . This latter feature implies that, rather than  $U$ , the velocity which determines the frequency of the oscillations is a combination of  $U$  and  $V_{cx}$  constant with  $U$  like  $V_r = V_{cx}/\alpha - U$ . Physically,  $-V_r$  represents a relative velocity of the flow and the cylinder.

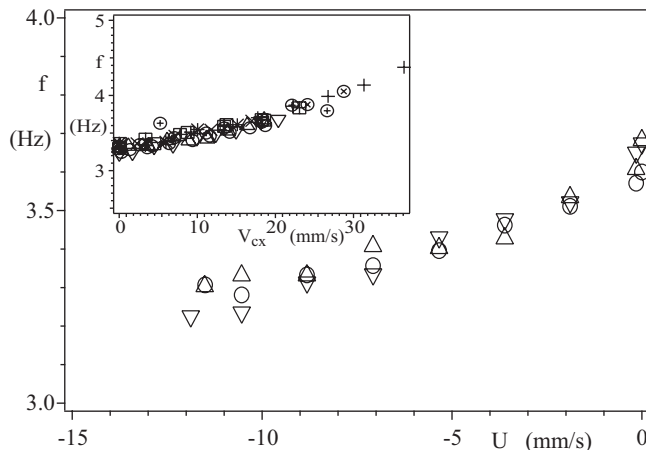


FIGURE 3 – Experimental variation of the transverse oscillation frequency as a function of the mean flow velocity  $U$  for free plexiglas cylinders of length  $L_c = 55$  mm and of different ratios  $D/H = 0.46$  ( $\nabla$ ),  $D/H = 0.53$  ( $\circ$ ),  $D/H = 0.56$  ( $\triangle$ ). The flowing fluid is a water-glycerol solution ( $C = 10\%$ ). Inset : variation of the oscillation frequency  $f$  as a function of  $V_{cx}$  for cylinders of diameter  $D = 1.5$  mm ( $D/H = 0.53$ ) and of different lengths :  $L_c = 10$  (+),  $20$  ( $\otimes$ ),  $30$  ( $\oplus$ ),  $40$  ( $\boxplus$ ),  $55$  ( $\circ$ ),  $60$  ( $\square$ ),  $70$  ( $\times$ ) and  $80$  mm (\*). Data points corresponding to  $D = 1.3$  mm ( $\nabla$ ) and  $D = 1.6$  mm ( $\triangle$ ) with  $L_c = 55$  mm have been added for comparison.

Rather than  $UH/\nu$ , the relevant Reynolds number of the process is therefore  $Re = V_r H/\nu$  which is constant with  $U$  for a given cylinder and fluid ; with this definition,  $Re$  becomes equal to  $UH/\nu$  only when the cylinder is at rest and  $V_{cx} = 0$ . The Reynolds numbers corresponding to the oscillations may be as low as  $Re \simeq 30$  (for  $D/H = 0.63$ ) : this value is well below those (100 or more) reported for vortex shedding behind fixed cylinders in similar confined geometries [3]. One deals therefore likely with a process different from vortex shedding : the coupling between the motion of the cylinder and the distortions of the flow field play here an important part. Together with these transverse oscillations, one observes, in addition, an angular oscillation of the cylinder around its axis at the same frequency  $f$  and a vertical oscillation at twice this frequency with respect to the mean global motion.

These features have been compared to those observed for tethered cylinders of same density, also between plane parallel walls and for  $D/H = 0.64$  [5]. In this case, too, transverse oscillations occur above a low threshold Reynolds number  $Re_c = 20$ ; the Reynolds number is defined as above by  $Re = UV_r/\nu$  and is, in this case, also equal to  $UH/\nu$  since  $V_{cx} = 0$ . For such tethered cylinders,  $f$  increases nearly linearly with the velocity  $U$  (*i.e.* with  $V_r$ ). Quantitatively, the Strouhal number  $S_r = fH/V_r$  decreases only by 20% as  $Re$  varies from 25 to 45 (Fig. 4). A similar trend is predicted by  $2D$  numerical simulations equivalent to the case  $L/W = 1$  (continuous line). This confirms that  $V_r$  is the relevant characteristic velocity : in the “free” case,  $V_r$  and  $f$  remain about constant as  $U$  varies while it is equal to  $U$  for tethered cylinders (so that  $f \propto U$ ).

This discussion is actually valid for a  $2D$  flow or when  $L_c = W$  : it has to be modified when  $L_c < W$  due to the flow  $U_a$  between the ends of the cylinder and the vertical sides of the cell (Fig. 1). Actually, the apparent weight of the free cylinders is balanced only by the hydrodynamic forces while, for tethered cylinders, the balance of forces involves in addition the tension of the suspension threads.

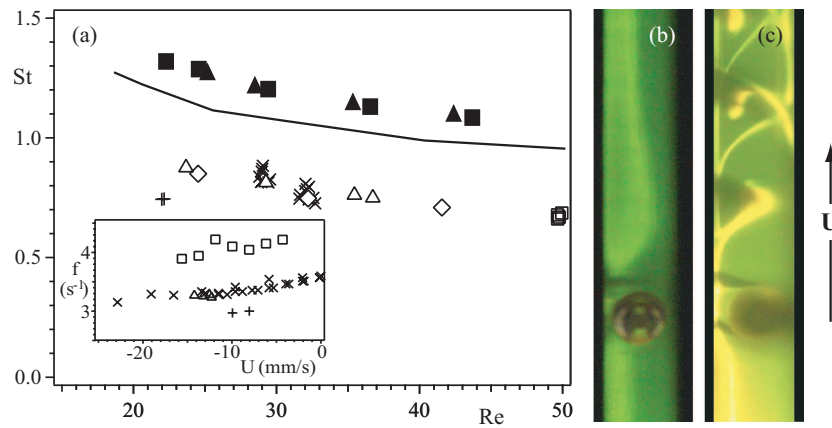


FIGURE 4 – a) Variations of the Strouhal number  $fH/V_r$  of the oscillations of plexiglas cylinders as a function of the Reynolds number  $Re$  for  $V_{cx} = 0$  - Free cylinder ( $L_c/W = 0.61$ ,  $D/H = 0.53$ ) ( $\diamond$ ) : water-glycerol solutions and ( $\triangle$ ) : water-salt-glycerol solutions of concentrations 0, 5, 10 and 15 % (the data points are in this order from right to left). Tethered cylinder :  $D/H = 0.64$ ,  $L_c/W = 0.98$  in water ( $\blacksquare$ ) and in solution  $WN$  ( $\blacktriangle$ ). Continuous line : numerical simulation. - Inset : variation with  $U$  of the frequency for water glycerol solutions of concentrations 0 % ( $\square$ ), 10 % ( $\times$ ), 20 % ( $+$ ) (these data are also plotted on the main graph). b)-c) Visualizations from the side of the cell of fluorescent dye injected upstream of a tethered cylinder kept fixed (b) or free to oscillate (c). The cell is illuminated by a laser sheet parallel to the  $(x, y)$  plane in the middle of the cell width.

For the tethered cylinder, visualisations have been performed by injecting a fluorescent dye upstream of the cylinder. At a same Reynolds number  $Re = 50$ , for a cylinder fixed (Fig. 4b) or free to move in the  $y$  direction (Fig. 4c), the dye streak is respectively straight or distorted by the oscillations.

### 3.3 Influence of the length of the cylinders

The transverse oscillations have been compared for cylinders of varying length ( $0.11 \leq L_c/W \leq 0.95$ ) with a constant diameter ( $D/H = 0.53$ ) and density ( $\rho_s = 1.19 \times 10^3 \text{ kg/m}^3$ ). As above, the velocity  $V_{cx}$  of the cylinder varies linearly with  $U$  : the slope of the variation is nearly constant with  $L_c/W$  ( $\alpha = 1.4 \pm 0.05$ ) while the relative velocity  $V_r$  increases monotonously for shorter cylinders. Transverse oscillations were observed for all values of  $L_c/W$  : their frequency  $f$  is remarkably independent of  $L_c$  and increases only slowly with  $V_{cx}$  (inset of Fig. 3).

These results suggest that, if  $L_c < W$ , the characteristic velocity determining the force on the cylinder and the frequency  $f$  is not the global combination  $V_r = V_{cx}/\alpha - U$  but a local relative velocity  $V_r^{local} = V_{cx}/\alpha - U^{local}$ .  $U^{local}$  is the local flow velocity above the cylinder with  $|U^{local}| < |U|$  : a part of the flow is indeed bypassed into the clearance of higher aperture between the ends of the cylinder and the sides (component  $U_a$  in Fig. 1). The velocity  $V_r^{local}$  must be independent of  $L_c/W$  due to the need to balance the apparent weight per unit length of the cylinder by the hydrodynamic force per unit length : this explains why  $f$  which depends on  $V_r^{local}$  rather than on  $V_r$  is also independent of  $L_c/W$ . In contrast, the velocity  $V_r$  increases (as observed experimentally) for lower ratios  $L_c/W$  because of the increasing influence of the bypass flow  $U_a$  :  $V_r$  is equal to  $V_r^{local}$  only in the limit :  $L_c \rightarrow W$ .

### 3.4 Influence of the fluid viscosity.

Experiments have been performed on free cylinders of constant diameter and length using liquids of different viscosities and densities. Using 10 % and 20 % water-glycerol solutions decreases the frequency  $f$  by up to 20 % compared to water (inset of Fig. 4) : however, for these solutions, both the viscosity and the density are changed by adding glycerol. Further comparisons were therefore performed between solutions with different glycerol concentrations, but with the density  $\rho_f = 1.035 \text{ g/cm}^3$  kept constant

by adding the proper amount of salt (Tab. 1) and  $U$  adjusted in order to have  $V_{cx} = 0$ .  $f$  is the same for all solutions although the viscosity (and therefore  $V_r$ ) varies ( $\Delta$  symbols in the inset).

For a tethered cylinder, one has compared results obtained using water and solution *NW* of different viscosity [5]. The frequency values are different but the two sets of data collapse when the Strouhal number  $St$  is plotted as a function of  $Re$  (main graph of Fig. 4). The data obtained for the free cylinder have been therefore also plotted in the same way (main graph of Fig. 4 : all the data obtained with water-glycerol solutions of concentration 0–15 % follow a same common trend similar to that discussed previously for the tethered cylinders. In this graph, the value of  $St$  for the tethered cylinders is about 30% higher than for free cylinders for a same value of  $Re$ . This difference may be partly due to the fact that both the vertical motion and the angular rotation with respect to the cylinder axis are blocked in the threaded case : the removal of the corresponding kinetic energy components will then change the frequency of the oscillation. The ratios  $L_c/W$  and  $D/W$  are also different in the two cases.

## 4 Conclusions

The experiments reported in the present paper show that both free and tethered horizontal cylinders submitted to a vertical flow between parallel plates display transverse oscillations down to Reynolds numbers  $Re$  as low as 20 : this instability was only observed for confinement ratios  $D/H$  between 0.46 and 0.63. This instability does not seem to correspond to vortex shedding which occurs for much larger  $Re$  values : rather, it involves a strong coupling between the displacement of the cylinder, the resulting distortions of the flow field and the pressure and shear forces induced on the cylinder [5].

The frequency  $f$  of the oscillations is determined by a relative velocity  $V_r$  of the fluid and the cylinder and not separately by their velocities  $U$  and  $V_{cx}$  : one has  $V_r = U - \alpha V_{cx}$  where  $\alpha$  is found independent of the diameter  $D$  of the cylinder and of its length  $L_c$ . For a tethered cylinder,  $V_r$  is equal to  $U$  since  $V_{cx} = 0$ ; for a free cylinder,  $V_r$  is instead independent of  $U$  because  $V_r$  determines the hydrodynamic force balancing the (constant) apparent weight of the cylinder. Using dimensionless Reynolds and Strouhal numbers  $Re$  and  $St$  based on the velocity  $V_r$  allows one to take into account the influence of the viscosity and density of the fluid since all frequency data collapse onto a single variation  $St(Re)$ .

The need to balance the weight of the cylinder by the hydrodynamic forces also explains the nearly constant value of  $f$  for free cylinders as  $L_c$  varies. Actually, rather than by  $V_r$ ,  $f$  is determined by the local relative velocity  $V_r^{loc} < V_r$  on the cylinder : the ratio  $V_r^{loc}/V_r$  increases towards 1 as  $L_c \rightarrow W$  when the effect of the bypass flow on the sides of the cylinder becomes lower.

Interestingly,  $f$  is also independent of the diameter for free cylinders at a given value of  $U$  : this may reflect combined effects of the variation of  $D$  on  $f$  and on  $V_r$ . Numerical  $2D$  simulations should help clear this point. In future work, it will be also important to investigate the  $3D$  fluttering oscillations which appear in addition to (or instead of) the transverse ones for  $D/H = 0.6$  and above.

## Références

- [1] D'Angelo M.V., Hulin J.P. and Auradou H. 2013 Oscillations and translation of a free cylinder in a viscous confined flow *Phys. Fluids* **25** 014102.
- [2] Richou A.B., Ambari A. and Naciri J.K. 2004 Drag force on a circular cylinder midway between two parallel plates at very low Reynolds numbers. Part 1 : Poiseuille flow (numerical) *Chem. Eng. Sci.* **59** 3215–3222. and Richou A. B., Ambari A., Lebey M. and Naciri J.K. 2005 Drag force on a cylinder midway between two parallel plates at  $Re \ll 1$ . Part 2 : moving uniformly (numerical and experimental) *Chem. Eng. Sci.* **60** 2535–2543.
- [3] Sahin M. and Owens R.G. 2004 A numerical investigation of wall effects up to high blockage ratios on two-dimensional flow past a confined circular cylinder *Phys. Fluids* **16** 1–25.
- [4] Semin B., Hulin J.P. and Auradou H. 2009 Influence of flow confinement on the drag force on a static cylinder *Phys. Fluids* **21** 103604.
- [5] Semin B., Decoene A., Hulin J.P., Francois M.L.M. and Auradou H. 2012 New oscillatory instability of a confined cylinder in a flow below the vortex shedding threshold. *J. Fluid Mech.* **690**, 345–365.